

Enhanced quantum sensing of gravitational acceleration constant

Giorgio Stucchi^{1,*} and Matteo G. A. Paris^{2,†}

¹*Max Planck Institute of Quantum Optics,*

Hans-Kopfermann-Str. 1, Garching 85748, Germany

²*Dipartimento di Fisica, Università di Milano, I-20133 Milan, Italy*

We investigate the use of quantum probes to accurately determine the strength of the local gravitational field on Earth. Our findings show that delocalized probes generally outperform localized ones, with the precision enhancement scaling quadratically with the separation between the two wavefunction components. This advantage persists under realistic position measurements, which can achieve precision not too far from the ultimate bound. We also discuss the influence of Earth's surface, demonstrating that its effect can be neglected until shortly before the particle hits the floor. Finally, we address the joint estimation of the gravitational acceleration g and the probe mass m , proving that the excess estimation noise arising from their inherent incompatibility is negligible.

I. INTRODUCTION

Over the past fifty years, there has been significant interest in exploring the relationship between quantum mechanics and gravity [1–6]. In the non-relativistic weak field regime, precise tests have been conducted to validate predictions based quantum mechanics and a Newtonian classical field. These experiments have successfully demonstrated that the dynamics of a quantum probe in a uniform gravitational field can be effectively described by a Schrödinger equation with a Hamiltonian incorporating a linear gravitational term as potential energy. This approach has enabled the prediction and measurement of gravitational effects on quantum systems using relatively simple experimental setups [7–9]. One of the pioneering experiments in this field was the COW experiment [10], which measured a gravitational effect in a quantum system. The experiment observed a phase-shift induced by gravity in a Mach-Zehnder interferometer using thermal neutrons. If the two arms of the interferometer are positioned at different heights, the wave-function accumulates a gravity-induced phase-shift that is absent when the interferometer is placed horizontally.

More recently, collaborations such as qBounce [11, 12] and GRANIT [13] have investigated ultracold neutrons confined by a perfect mirror. These neutrons serve as ideal probes due to

* giorgio.stucchi@tum.de

† matteo.paris@fisica.unimi.it

their light mass and null electric charge. In addition to the gravitational potential, the particles also experience an infinite barrier at the origin. The dynamics of these quantum bouncers have been explored theoretically and experimentally. Ultracold neutrons provide a very useful tool to investigate gravitational phenomena in the quantum regime [14, 15], and can be used as test of interactions beyond the Standard Model and General Relativity in the qBOUNCE and GRANIT experiments, for example as a tool for probing of beyond-Riemann gravity [16], or influence of a spontaneous Lorentz symmetry breaking on the gravitational quantum states of the ultracold neutrons [17]. Experiments have also been proposed and conducted to examine the free fall of antimatter particles [18], as the GBAR experiment [19].

The coupling of a quantum probe to gravity also gives the opportunity to estimate the gravitational acceleration, which in turn may provide constraints on any possible gravity-like interaction at a given interaction range [20, 21]. Indeed, the phase difference accumulated in an interferometer [22], or the discrete energy spectrum of a quantum bouncer [23] do depend on the value of g . We thus aim to determine the fundamental limits to the precision in the estimation of g [24, 25], and how it is possible to achieve such ultimate bounds. In particular, we want to assess the use of superpositions of states rather than localized ones.

Our findings show that delocalized probes generally outperform localized ones, with the precision enhancement scaling quadratically with the separation between the two wavefunction components. This advantage persists under realistic position measurements, which can achieve precision not too far from the ultimate bound. Concerning the influence of Earth's surface, we prove that its effect can be neglected in a first approximation. We also address the joint estimation of the gravitational acceleration g and the mass m of the quantum probe, proving that there is no excess estimation noise arising, despite their inherent incompatibility as parameters.

The paper is structured as follows. In Sections II and III we briefly review the tools of quantum estimation theory and the quantum description of a free falling body and a quantum bouncer, respectively. In Section IV we derive the ultimate quantum bound to precision in the estimation of g for a localized probe as well as for superpositions, showing that delocalized probes provide a precision enhancement scaling quadratically with the separation between the two wavefunction components. In Section V we prove that there is a large temporal range in which the influence of Earth's surface can be neglected, validating the results of Section IV. In Section VI we study the performance of position measurements, showing that the advantage of superpositions persists, and that the Fisher information is not much smaller than the QFI. Finally, in Section VII we discuss joint estimation of the gravitational acceleration and the probe mass, proving that the excess estimation

noise arising from their inherent incompatibility is negligible. Section VIII closes the paper with some concluding remarks.

II. CLASSICAL AND QUANTUM ESTIMATION THEORY

In classical estimation theory, the central challenge lies in estimating an unknown parameter, denoted as λ , given a set of outcomes x_1, x_2, \dots, x_M from a set of experimental data distributed according to a conditional probability distribution $p(x|\lambda)$. Given λ and a sample space $\chi = \{x\}$, namely a subset of all possible outcomes of the experiment, an estimator $\hat{\lambda}$ is a function from the sample space χ to the space of the possible values of λ . The variance $\text{Var}(\hat{\lambda})$ of any unbiased estimator $\hat{\lambda} = \hat{\lambda}(x_1, x_2, \dots, x_M)$ satisfies the Cramér-Rao inequality [26]:

$$\text{Var}(\hat{\lambda}) \geq \frac{1}{MF(\lambda)}, \quad (1)$$

where $F(\lambda)$ is the Fisher Information (FI) defined as:

$$F(\lambda) = \int dx p(x|\lambda) \left(\frac{\partial \log(p(x|\lambda))}{\partial \lambda} \right)^2. \quad (2)$$

According to the Cramér-Rao bound the optimal measurement to estimate the quantity λ is the one with conditional distribution $p(x|\lambda)$ that maximizes the Fisher Information. On the other hand, for any fixed measurement an efficient estimator is an estimator that saturates the Cramér-Rao inequality [27].

For quantum systems, any estimation problem can be formulated by considering a family of quantum states ρ_λ defined on a specific Hilbert space \mathcal{H} . To estimate the value of λ , measurements are performed on the quantum state ρ_λ followed by classical data processing on the measurement results [28, 29]. Introducing the Symmetric Logarithmic Derivative (SLD) L_λ as the self-adjoint operator satisfying the equation $\frac{1}{2}(L_\lambda \rho_\lambda + \rho_\lambda L_\lambda) = \partial_\lambda \rho_\lambda$, the following inequality can be obtained:

$$\text{Var}(\hat{\lambda}) \geq \frac{1}{MH(\lambda)}, \quad (3)$$

where the Quantum Fisher Information (QFI) is defined as $H(\lambda) = \text{Tr}[\rho_\lambda L_\lambda^2]$ and is always greater than or equal to the FI of any measurement procedure. The spectral measure of the SLD represents the optimal measurement to be performed on the system, i.e. the measurement with a FI equal to the QFI.

For a generic family of pure states the QFI is given by

$$H(\lambda) = 4[\langle \partial_\lambda \psi_\lambda | \partial_\lambda \psi_\lambda \rangle - |\langle \partial_\lambda \psi_\lambda | \psi_\lambda \rangle|^2]. \quad (4)$$

If the parameter is encoded on the quantum system via a parameter-dependent unitary transformation U , we introduce the Hermitian operator

$$\mathcal{G} := i(\partial_\lambda U^\dagger)U, \quad (5)$$

and the QFI can be expressed as [30]

$$H(\lambda) = 4 [\langle \psi_0 | \mathcal{G}^2 | \psi_0 \rangle - \langle \psi_0 | \mathcal{G} | \psi_0 \rangle^2]. \quad (6)$$

In other words, the QFI is proportional to the variance of \mathcal{G} on the initial state $|\psi_0\rangle$. For a parametrization transformation of the form $U = \exp(-itJ_\lambda)$, where \hbar has been set as 1, \mathcal{G} can be expressed as

$$\mathcal{G} = - \int_0^t ds e^{isJ_\lambda} (\partial_\lambda J_\lambda) e^{-isJ_\lambda}. \quad (7)$$

A. Multiparameter Quantum Estimation

The dynamics of a system are often influenced by multiple interconnected parameters. However, extending results such as the Cramér-Rao bound to the multiparameter case is not straightforward, because the optimal measurement strategy for one parameter may not commute with the optimal scheme for another parameter. This incompatibility between measurements arises from fundamental principles in quantum mechanics. Furthermore, when a measurement is fixed, correlations can emerge among the parameters. Consequently, trade-off relations among the uncertainties of the parameters arise, as the initial information in the measurement probe needs to be distributed among the different parameters [31, 32].

Similarly to the single parameter case, symmetric logarithmic derivative (SLD) operators L_μ may be introduced for each parameter, and the so-called QFI matrix may be constructed, with elements

$$H_{\mu\nu}(\boldsymbol{\lambda}) = \text{Tr} \left[\rho_{\boldsymbol{\lambda}} \frac{L_\mu L_\nu + L_\nu L_\mu}{2} \right], \quad (8)$$

leading to a matrix quantum Cramér-Rao bound $\mathbf{V}(\hat{\boldsymbol{\lambda}}) \geq \mathbf{H}(\boldsymbol{\lambda})^{-1}$ where \mathbf{V} is the mean square error matrix (the covariance matrix for unbiased estimators). This relation is of little use, since no ordering is available for matrices. To get a better insight into the performance of different multiparameter estimators, it is convenient to introduce a weight matrix \mathbf{W} (positive, real matrix of dimension $d \times d$) and recast the matrix bound into a scalar bound as follows

$$\text{Tr} [\mathbf{WV}] \geq \text{Tr} [\mathbf{WH}^{-1}] \equiv C^S(\mathbf{W}). \quad (9)$$

This bound is in general not attainable, due to the possible non-commutativity of the different SLD operators [31]. Holevo derived a tighter scalar bound $C^H(\boldsymbol{\lambda}, \mathbf{W})$ via explicit minimization [29], which can be achieved by collective measurements on an asymptotically large number of copies of the state. Closed form expressions of the Holevo bound are hard to obtain, but it can be upper- and lower bounded as follows:

$$C^S(\mathbf{W}) \leq C^H \leq (1 + \mathcal{R}) C^S(\mathbf{W}), \quad (10)$$

where the quantity \mathcal{R} is defined as

$$\mathcal{R} = \|i\mathbf{H}^{-1}\mathbf{D}\|_{\infty} = \sqrt{\frac{\det \mathbf{D}}{\det \mathbf{H}}} \quad (11)$$

where $\|\mathbf{A}\|_{\infty}$ denotes the largest eigenvalue of the matrix \mathbf{A} , and the second equality is valid only for statistical models with two parameters. The matrix \mathbf{D} is the Uhlmann curvature, with elements

$$D_{\mu\nu} = -\frac{i}{2} \text{Tr} [\rho_{\lambda} [L_{\mu}^S, L_{\nu}^S]] . \quad (12)$$

The quantity \mathcal{R} satisfies the constraint $0 \leq \mathcal{R} \leq 1$, and provides a general bound, independent on the choice of the weight matrix. If a specific weighting is more appropriate for the statistical model at hand, a more refined bound may be obtained as follows

$$C^S(\mathbf{W}) \leq C^H \leq [1 + \mathcal{T}(\mathbf{W})] C^S(\mathbf{W}), \quad (13)$$

where

$$\mathcal{T}(\mathbf{W}) = \frac{\|\sqrt{\mathbf{W}}\mathbf{H}^{-1}\mathbf{D}\mathbf{H}^{-1}\sqrt{\mathbf{W}}\|_1}{C^S(\mathbf{W})} = \frac{2\sqrt{w \det \mathbf{D}}}{H_{11} + wH_{22}} \quad (14)$$

with $\|\mathbf{A}\|_1$ denoting the sum of the singular values of the matrix \mathbf{A} , and the second equality valid only for statistical models with two parameters and diagonal weight matrix $\mathbf{W} = \text{Diag}(1, w)$.

III. FALLING QUANTUM PARTICLES

A. Quantum free fall

The idealized system is given by a quantum particle evolving in a uniform gravitational field, i.e. in a potential $V(x) = mgx$. This coincides with the first order expansion of the Newtonian potential $\tilde{V}(x) = -\frac{GMm}{(R+x)^2}$ after substitution of $g = \frac{GM}{R^2}$, having denoted with x the distance from the floor, with M and R the mass and radius of the Earth respectively, and with G the gravitational

constant. The approximation consists in neglecting the presence of the floor. The Hamiltonian of the system is given by [33, 34]

$$\mathcal{H} = \frac{p^2}{2m} + mgx. \quad (15)$$

The t-independent Schrödinger equation reads:

$$\left\{ -\frac{\hbar}{2m} \left(\frac{d}{dx} \right)^2 + mgx \right\} \Psi(x) = E\Psi(x) \quad (16)$$

Introducing the shifted and re-scaled new independent variable $y = k(x - \frac{E}{mg})$ and adopting the notation $\Psi(x) = \sqrt{k}\psi(y)$, with $k = (\frac{2m^2g}{\hbar^2})^{\frac{1}{3}}$, the differential equation then simply becomes

$$\frac{d^2}{dy^2} \psi(y) = y\psi(y) \quad (17)$$

Eq. (17) is Airy's differential equation: its solutions are linear combinations of the *Airy functions* $\text{Ai}(y)$ and $\text{Bi}(y)$, of which (since $\text{Bi}(y)$ diverges as $y \rightarrow \infty$) only the former

$$\text{Ai}(y) \equiv \frac{1}{\pi} \int_0^\infty du \cos\left(yu + \frac{1}{3}u^3\right) \quad (18)$$

are selected. These solutions are only improperly normalizable: by imposing that

$$\int_{-\infty}^\infty dx \psi(y)\psi^*(y) = \delta(E - E') \quad (19)$$

one finds the final expression for the energy eigenfunctions [35]:

$$\Psi_E(x) = \frac{(2m)^{\frac{1}{3}}}{\hbar^{\frac{2}{3}}(mg)^{\frac{1}{6}}} \text{Ai}\left(k\left(x - \frac{E}{mg}\right)\right). \quad (20)$$

The energy spectrum is continuous, and has no least member: the system possesses no ground state. The eigenfunctions $\Psi_E(x)$ comprise a complete orthonormal set [36]. With them, the propagator can be constructed

$$K(x_1, t_1; x_0, t_0) = \int_{-\infty}^\infty dE \Psi_E(x_1) \Psi_E^*(x_0) e^{-\frac{i}{\hbar} E(t_1 - t_0)} \quad (21)$$

which allows one to describe the dynamical evolution of any prescribed initial state:

$$\begin{aligned} |\psi_t\rangle &= e^{-\frac{i}{\hbar} \mathcal{H}t} |\psi_0\rangle \\ |\psi_0\rangle &= \int dx \psi(x, 0) |x\rangle \\ |\psi_t\rangle &= \int dx \psi(x, t) |x\rangle \\ \psi(x, 0) &\mapsto \psi(x, t) = \int dx_0 K(x, t; x_0) \psi(x_0, 0) \end{aligned} \quad (22)$$

Eq. (21) yields [36]

$$K(x, t; x_0) = \sqrt{\frac{m}{2\pi i \hbar t}} \exp\left[\frac{i}{\hbar} \left(\frac{m}{2t}(x - x_0)^2 - \frac{1}{2} mgt(x + x_0) - \frac{1}{24} mg^2 t^3\right)\right] \quad (23)$$

B. Quantum Bouncer

Let us now consider the presence of the Earth's surface. The potential is obtained by erecting an impenetrable barrier at the coordinate origin, the intended effect of which is to render inaccessible the points with $x < 0$ [23, 37–39].

$$V(x) = \begin{cases} \infty & \text{if } x < 0, \\ mgx & \text{if } x \geq 0. \end{cases} \quad (24)$$

The t-independent Schrödinger equation is the same as for the free fall, but in this case it is required that

$$\Psi(x < 0, t) = 0 \quad \forall t. \quad (25)$$

This amounts to a requirement that the probability current $i \frac{\hbar^2}{2m} (\Psi^* \Psi - \Psi \Psi^*)|_{x=0} = 0 \quad \forall t$, which is achieved by imposing the boundary condition

$$\Psi(0, t) = 0 \quad \forall t. \quad (26)$$

The presence of this boundary condition is what sets the two problems apart, and it is a crucial factor. It leads to a discrete energy spectrum, ensures that the eigenfunctions are normalizable, and provides the system with a ground state, which was absent in the case of free fall [36]. Just as in the free fall, the eigenfunctions have the form

$$\Psi(x) \propto \text{Ai}(k(x - a)) \quad (27)$$

and to achieve compliance with the boundary condition (26), $a \equiv \frac{E}{mg}$ must be assigned such a value as to make $-ka$ coincide with a zero, which is denoted as $-z_n$, of the Airy function. Hence $a_n = z_n/k$, and thus the energy eigenvalues are:

$$E_n = \frac{mgz_n}{k} \quad n = 1, 2, 3, \dots \quad (28)$$

The associated eigenfunctions are

$$\Psi_n(x) = \mathcal{N}_n \text{Ai}(kx - z_n) \quad (29)$$

where \mathcal{N}_n is a normalization factor, defined by the condition

$$\int_0^\infty [\Psi_n(x)]^2 dx = \mathcal{N}_n^2 \cdot \int_0^\infty [\text{Ai}(kx - z_n)]^2 dx \quad (30)$$

Hence

$$\mathcal{N}_n = \sqrt{k} \left[\int_0^\infty [\text{Ai}(z - z_n)]^2 dz \right]^{-\frac{1}{2}} \quad (31)$$

where $z = kx$. This can be simplified further [35]:

$$\mathcal{N}_n = \sqrt{k} [\text{Ai}'(-z_n)]^{-1} \quad (32)$$

In this setting, calculating the propagator analytically is unfeasible. Therefore, the dynamically evolved wave packet is conveniently described by

$$\Psi(x, t) = \sum_n c_n \Psi_n(x) e^{-\frac{i}{\hbar} E_n t} \quad (33)$$

$$c_n = \int_0^\infty \Psi_n(\xi) \Psi(\xi, 0) d\xi. \quad (34)$$

C. Static estimation of g using stationary quantum probes

In recent experiments, eigenstates of the quantum bouncer have been generated [40, 41] and a question arises on whether they provide a mean to encode and retrieve information on g . We anticipate that being based on stationary states this estimation strategy cannot be improved by dynamical encoding and the QFI is constant in time. Using Eqs. (29) and (4) we arrive at

$$H^{(n)}(g) = \frac{1}{7g^2} \left(1 + \frac{32z_n^3}{135} \right), \quad (35)$$

where $-z_n$ is the n -th zero of the Airy function. Preparing eigenstates with larger energy would be thus advantageous for the estimation of g . Remarkably, if we compute the FI for position measurements, i.e., the FI in Eq. (2) for the distribution $|\psi_n\rangle$ we obtain the same results. This means that position measurement is optimal to estimate g when this parameter is encoded onto energy eigenstates. In order to obtain a dynamical advantage, i.e., to exploit the encoding of g due to evolution, we may consider superpositions of energy eigenstates. However, these kind of probes are challenging to produce [42] and we prefer to address dynamical estimation for more realistic preparations.

IV. ESTIMATION OF g BY FREE FALLING QUANTUM PROBES

We now analyze whether the parameter g may be estimated by performing measurements on a free falling quantum probe, and focus on whether using a superposition of Gaussian packets, instead

of a localized one, is beneficial from the point of view of extracting information from the system. We will be using natural units, with $\hbar = 1$ and $c = 1$.

To calculate the QFI for the parameter g in the no-floor regime, we use formula (6), since we are working with pure states under unitary transformations. The initial ($t = 0$) state is described by the wavefunction

$$\psi_0(x) \equiv \psi(x, 0) = \frac{1}{(2\pi\sigma^2)^{1/4}} \exp\left(-\frac{x^2}{4\sigma^2}\right) \quad (36)$$

In order to evaluate Eq. (7) for our system, we make use of the Baker-Campbell-Hausdorff formula and from Eq. (7) we find the operator

$$\mathcal{G} = -(mtx + \frac{t^2}{2}p).$$

The QFI is then given by 4 times the variance of \mathcal{G} on the initial state. Alternatively, upon observing that the propagator in Eq. (21) is symmetric in its arguments $K(x, t; x_0) = K(x_0, t; x)$ and its derivative is given by

$$\partial_g K(x, t; x_0) = -\frac{i}{2}mt \left(\frac{1}{6}gt^2 + x + x_0 \right) K(x, t; x_0),$$

the QFI may be expressed in terms of the fluctuations of the position operator on the evolved state as

$$H(g) = 4m^2t^2 \left(\langle \psi_t | x^2 | \psi_t \rangle - \langle \psi_t | x | \psi_t \rangle^2 \right). \quad (37)$$

Either way, for a localized initial state $|\psi_0\rangle$ we find

$$H_{loc} = \frac{t^4}{4\sigma^2} + 4m^2t^2\sigma^2, \quad (38)$$

which is independent on g itself. The same results is obtained if the probe has an initial momentum, i.e. if the initial wave function is $\psi_0(x, 0)e^{ip_0x}$. The QFI increases for decreasing σ , i.e. if the particle is more localized. The QFI scales as t^2 for short times whereas asymptotically (for large times) we have $H_{loc} \propto t^4$. The emergence of this scaling may be strongly delayed if σ is large, as the first term in Eq. (38) becomes larger than the second only for $t > 4m\sigma^2$.

Let us now consider a particle initially prepared in a superposition of two Gaussian wavepackets, placed at distance $2a$ each other, and having opposite momenta $\pm p_0$ with $p_0 > 0$ (i.e. the wavepacket on the right has positive momentum and viceversa)

$$\psi(x, 0) = \frac{e^{-\frac{(x-a)^2}{4\sigma^2} + ip_0x} + e^{-\frac{(x+a)^2}{4\sigma^2} - ip_0x}}{A^{\frac{1}{2}} (2\pi\sigma^2)^{\frac{1}{4}}} \quad (39)$$

$$A = 2 \left(1 + e^{-\frac{(a^2 + 4p_0^2\sigma^4)}{2\sigma^2}} \right) \quad (40)$$

In this case, the QFI of the evolved state may be written as

$$\begin{aligned}
H_{sup} = & H_{loc} + 8 m^2 \sigma^2 t^2 \left[\frac{a^2}{2\sigma^2} - g(a, \sigma, p_0) \right] \\
& + 4 a m p_0 t^3 + \frac{t^4}{2\sigma^2} \left[2\sigma^2 p_0^2 - g(a, \sigma, p_0) \right], \\
g(a, \sigma, p_0) = & \frac{\frac{a^2}{2\sigma^2} + 2\sigma^2 p_0^2}{1 + \exp(\frac{a^2}{2\sigma^2} + 2\sigma^2 p_0^2)}.
\end{aligned} \tag{41}$$

From Eq. (41) it is clear that for $a^2 > 2\sigma^2\mu$ and $p_0^2 > \mu/2\sigma^2$, where $\mu = \max_x e^x/(1+e^x) \simeq 0.278$, i.e. for particles that are enough *fast and delocalized* compared to the wavepackets width, one has $H_{sup} > H_{loc}$, in agreement with the intuition suggested by Eq. (37). For the special cases $a = 0$ (initially localized particle, with two opposite momenta) and $p_0 = 0$ (initially delocalized particle with no momentum) we have

$$\begin{aligned}
H_{sup} = & H_{loc} + \frac{1}{2} t^4 p_0^2 (1 + \tanh \sigma^2 p_0^2) \\
& - \frac{1}{2} t^2 p_0^2 m^2 \sigma^4 (1 - \tanh \sigma^2 p_0^2)
\end{aligned} \tag{42}$$

$$\begin{aligned}
H_{sup} = & H_{loc} + 2a^2 m^2 t^2 \left(1 + \tanh \frac{a^2}{4\sigma^2} \right) \\
& + \frac{a^2 t^4}{8\sigma^2} \left(1 - \tanh \frac{a^2}{4\sigma^2} \right)
\end{aligned} \tag{43}$$

The first expression shows that for an initially localized particle with two opposite momenta, we gain precision for large times, whereas the second ensures that even without an initial momentum, the use of a delocalized probe always provides enhanced precision compared to a localized one. The precision enhancement scales as the square of the separation between the two wavepackets. Notice that for large times, i.e. when the term proportional to t^4 in Eq.(43) is dominant, the QFI enhancement is maximized for a specific ratio between a^2 and σ^2 i.e. for $a^2 = 4\xi\sigma^2$ where $\xi = \arg \max x(1 - \tanh x) \simeq 0.64$ is the value of x maximizing the function $x(1 - \tanh x)$.

Summarizing, the use of quantum probes (superpositions) generally enhances precision in the estimation of the strength of the local gravitational field of Earth. Precision may be optimized by mild state engineering.

V. FREE FALLING VS QUANTUM BOUNCER

We now consider the presence of the Earth surface and analyze the dynamics of a *quantum bouncer* [43–46]. Our goal is to assess whether the *no floor* approximation is valid for a certain range of time before the particle hits the Earth. We anticipate that this is indeed the case, thus

justifying the use of the free-falling model, and validating the results about the QFI obtained in the previous Section.

The initial states are those given in Eqs. (36) and (39), the only difference being that the wave packets are now translated to take into account the initial height h from the floor. Notice that strictly speaking those states are not normalized on $(0, \infty)$. However, for $h \gg \sigma$ (i.e., assuming that the wave packet is dropped from a height large compared to its width) they are nearly normalized (and in particular the wavefunction vanishes at the Earth surface).

As a matter of fact, the dynamics cannot be studied analytically and we use Eqs. (33) and (34) to evaluate the evolved states of the quantum bouncer, and Eq. (4) to calculate the QFI numerically. To contain the computational load, we focus on situations where about ≈ 100 coefficients in Eq. (36) are enough to describe the dynamics. This corresponds to regimes where the combination of parameters $k = (\frac{2m^2g}{\hbar^2})^{\frac{1}{3}}$ is of the order of one. The comparison between the QFI $H(g)$ obtained with and without considering the presence of Earth's surface is shown in Fig. 1, for initially localized wavepackets. Similar results may be obtained for superpositions.

Figure 1 displays comforting results: there is a large time range where the behaviour of the QFI is exactly the same as in the no-floor approximation. This means that until shortly before the particle hits the floor, it is as if the floor wasn't there at all.

VI. ESTIMATION OF g BY POSITION MEASUREMENT

We now consider a realistic measurement procedure, i.e., the measurement of the position of the particle, that may be performed in order to estimate g . Our aim is to assess the use of superpositions and to benchmark its precision by comparing the position FI to the QFI. To calculate the FI, we make use of the propagator in Eq. (23) to find the evolved state from Eq. (22). For a localized Gaussian wavepacket we obtain

$$\begin{aligned} \psi(x, t) &= \frac{(1+i)\sqrt{m\sigma}}{(2\pi)^{\frac{1}{4}}\sqrt{t+2im\sigma^2}} \\ &\times \exp \left\{ -\frac{m \left[x^2 - xgt(t-4im\sigma^2) - \frac{1}{12}g^2t^3(t-8im\sigma^2) \right]}{2(it+2m\sigma^2)} \right\} \end{aligned} \quad (44)$$

For position measurement, the probability distribution $p(x|g)$ that we need to use Eq. (2) is immediately given by $|\psi(x, t)|^2$ with $\psi(x, t)$ given above. Plugging $|\psi(x, t)|^2$ and its derivative with respect to g into Eq. (2), we obtain the FI for position measurements:

$$F_{x,loc}(g) = \frac{m^2t^4\sigma^2}{t^2 + 4m^2\sigma^4}. \quad (45)$$

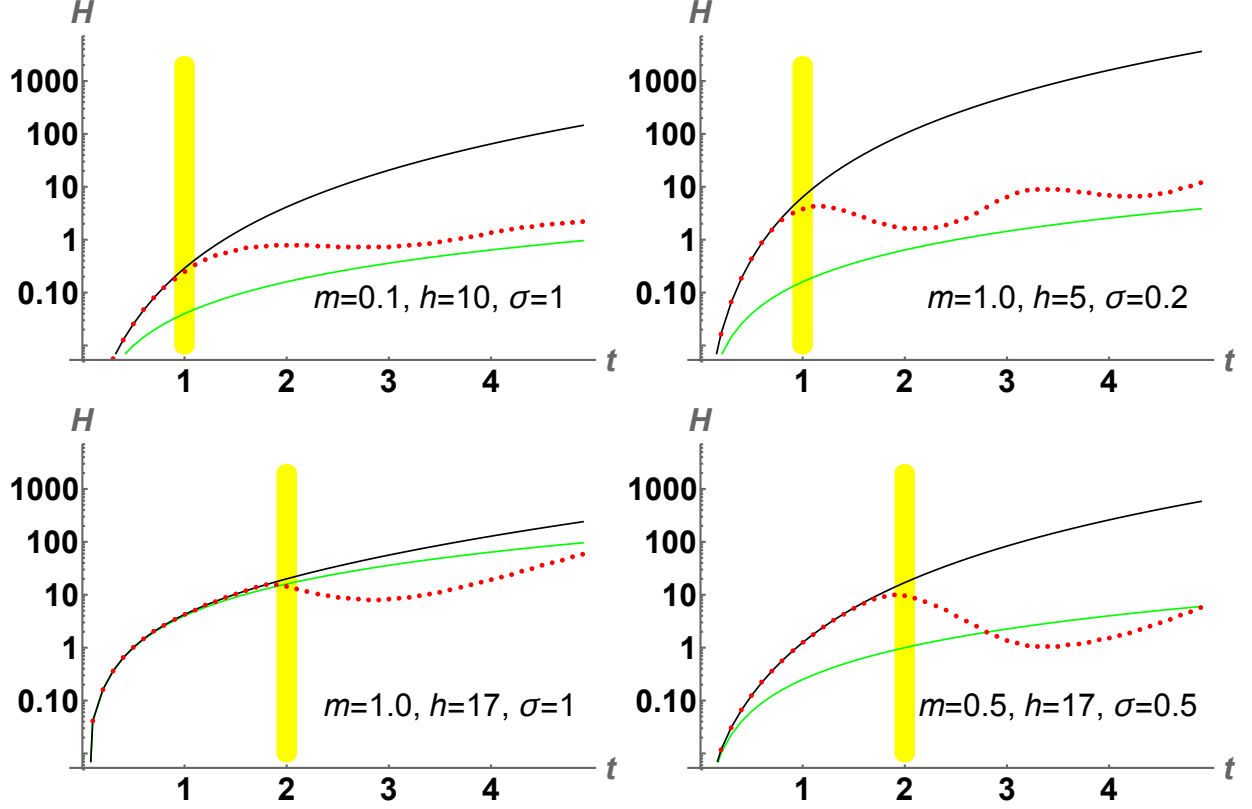


Figure 1. QFI $H(g)$ for the estimation of g by a quantum bouncer (red points) compared to the same quantity obtained with a free falling probe (black solid lines) for different values of the involved parameters. The green line denotes the t^2 term of the no-floor QFI. The yellow columns provide a visual aid to discern the end of the range of validity of the no-floor approximation.

We notice that the dependence on the parameters of the position FI in Eq. (45) is different from that of the QFI, e.g., the value $\sigma = \frac{\sqrt{t}}{2\sqrt{m}}$, which minimizes the QFI, is now the one maximizing the FI.

Also in this case, we are interested in assessing whether using superpositions of localized states provides some advantages. The explicit expression of the position FI is clumsy and will not be reported here. Extensive numerical analysis shows that a convenient working regime is achieved for superpositions of highly localized states (i.e., for small σ) while the initial momentum is not much relevant.

In Fig. 2 we show the two ratios

$$\gamma_S = \frac{F_{x,sup}}{F_{x,loc}} \quad \gamma_H = \frac{F_{x,sup}}{H_{sup}} \quad (46)$$

as a function of the separation a for various values of σ . The other parameters are set to $t = 1.0$ and $m = 0.5$ in order to safely stay within the no-floor approximation. The ratio γ_S quantifies the

gain one obtains using superpositions instead of localized probes, whereas γ_H assess the precision of position measurement against the ultimate bounds imposed by quantum mechanics.

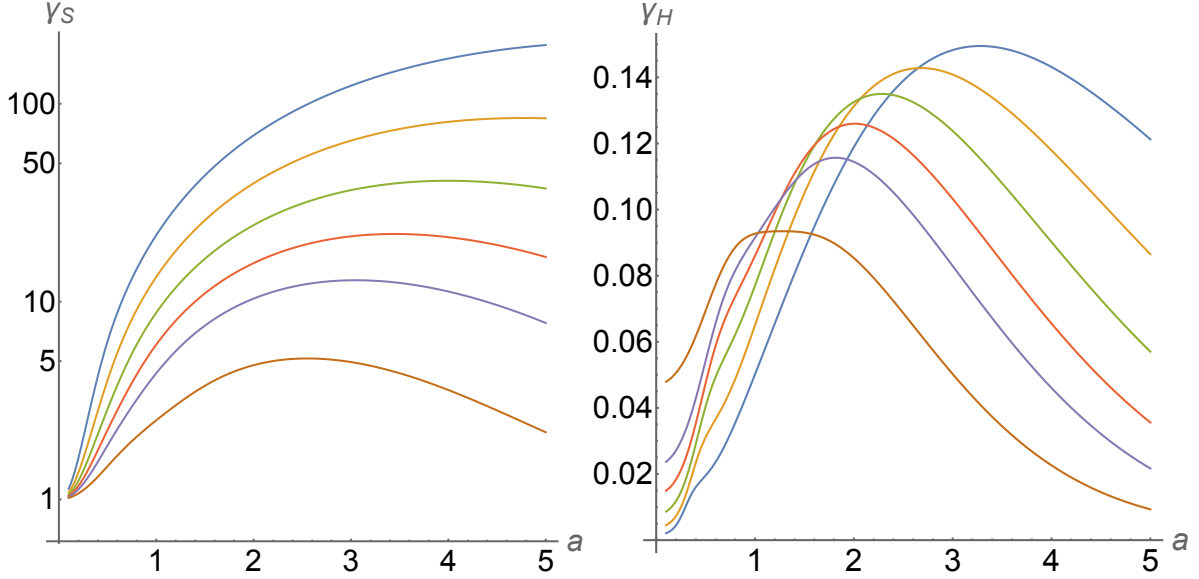


Figure 2. (Left): the ratio γ_S between the FI of position measurement for probes prepared in a superposition state and that obtained for localized probes, as function of the separation a and for different values of the wavepackets width σ . From top to bottom: $\sigma = 0.2, 0.25, 0.3, 0.35, 0.4, 0.5$. (Right): the ratio γ_H between the FI of position measurement for probes prepared in a superposition state and the corresponding QFI, as function of the separation a and for different values of the wavepackets width σ . From top to bottom: $\sigma = 0.2, 0.25, 0.3, 0.35, 0.4, 0.5$. In both plots, the other parameters are set to $t = 1.0$ and $m = 0.5$ in order to safely stay within the no-floor approximation.

The plots show that the use of superpositions is largely advantageous, especially for lower values of σ , and that the Fisher information of position measurement is a consistent fraction of the QFI.

VII. JOINT ESTIMATION OF g AND m

In the previous Sections, we have seen that the precision in the estimation of g is determined by the values of the other parameters. Focusing for simplicity on the case of a localized probe, those parameters are the interaction time t , the width σ of the wavepacket, and the mass of the particle m . The first two parameters may be tuned by the experimenter while the mass of the particle should be determined independently and assumed to stay constant during the repeated preparations of the probe. This assumption, and the related risk of introducing systematic errors, may be avoided by performing the joint estimation of g and m . In this Section, we consider the problem of estimating

g and m simultaneously, and investigate whether they are compatible parameter [47], i.e., whether the joint estimation introduces additional quantum noise.

We start by calculating the QFI matrix and the Uhlmann curvature using Eq.s (A1) and (A2).

$$\mathbf{H}(g, m) = 4 \begin{pmatrix} H_{loc} & \frac{g}{m} \left(H_{loc} - \frac{t^2}{4\sigma^2} \right) \\ \frac{g}{m} \left(H_{loc} - \frac{t^2}{4\sigma^2} \right) & \frac{t^2}{8m^4\sigma^4} + \frac{g^2 t^4}{m^2\sigma^2} + 4g^2\sigma^2 \end{pmatrix} \quad (47)$$

$$\mathbf{D}(g, m) = 4 \begin{pmatrix} 0 & gt^3 \\ -gt^3 & 0 \end{pmatrix}. \quad (48)$$

Eq. (48) proves that the two parameters are not compatible, since the corresponding SLDs do not commute on the relevant subspace. On the other hand, upon calculating the quantities \mathcal{R} and $\mathcal{T}(\mathbf{W})$ we have

$$\mathcal{R} = \frac{4\sqrt{2}gm^2t\sigma^3}{\sqrt{16m^2\sigma^4 + t^2(1 + 32g^2m^4\sigma^6)}} \quad (49)$$

$$\mathcal{T}(\mathbf{W}) = \frac{16gm^4t\sqrt{w}\sigma^4}{w + 2m^2t^2\sigma^2(m^2 + 4g^2w) + 32m^4\sigma^6(m^2 + g^2w)}, \quad (50)$$

and substituting a sensible choice of parameters (in natural units) $g \simeq 2.15 \cdot 10^{-32}$ GeV, $m \simeq 10$ a.m.u $\simeq 9.31$ GeV, $\sigma \simeq 10^{-3} m \simeq 5.1 \cdot 10^{-6}$ GeV $^{-1}$, we found that $\mathcal{R} \simeq \mathcal{T}(\mathbf{W}) < 10^{-40} \forall t$ and $\forall w$.

Additionally, by choosing $w = 0$ we have $\mathcal{T}(\mathbf{W}) = 0$ and we can compare precision achievable in estimating g knowing m (given by $1/H_{loc}$) with that achievable without any knowledge of m (treated as a nuisance parameter). For the same set of parameters we have $1/H_{loc} \simeq (\mathbf{H}^{-1})_{11}$, confirming that the quantum noise due to incompatibility is negligible.

VIII. CONCLUSIONS

In this work, we have investigated the potential of quantum probes in enhancing the precision in the estimation of the gravitational acceleration constant g . Our results demonstrate that delocalized quantum probes, prepared in superposition states, generally outperform localized ones, with the precision enhancement scaling quadratically with the separation between the wavefunction components. This advantage persists also under realistic position measurements, where the Fisher information remains close to the ultimate quantum bound set by the quantum Fisher information.

We have validated the no-floor approximation for a large temporal range, showing that the influence of Earth's surface is negligible until shortly before the probe interacts with it. Furthermore, we have addressed the joint estimation of g and of the probe mass m , proving that despite their inherent incompatibility as parameters, only negligible excess noise is introduced. This result

ensures that simultaneous estimation does not degrade precision, making it a viable strategy in implementations. Our findings highlight the potential of quantum-enhanced sensing in gravitational measurements, with applications in fundamental physics and precision metrology [48–52].

ACKNOWLEDGMENTS

MGAP thanks Massimo Frigerio, Carlo Cepollaro, Flaminia Giacomini, Luigi Seveso, and Valerio Peri for interesting and useful discussions.

Appendix A: Quantumness of two-parameter models

For a generic two-parameter pure state model $|\psi_{\boldsymbol{\lambda}}\rangle$, with $\boldsymbol{\lambda} = (\lambda_1, \lambda_2)$, the QFI matrix and the Uhlmann curvature can be evaluated via the following equations [53]:

$$\mathbf{H}(\boldsymbol{\lambda}) = 4 \begin{pmatrix} a^2 + \alpha & ab + \text{Re}(c) \\ ab + \text{Re}(c) & b^2 + \beta \end{pmatrix}, \quad (\text{A1})$$

$$\mathbf{D}(\boldsymbol{\lambda}) = 4 \begin{pmatrix} 0 & \text{Im}(c) \\ -\text{Im}(c) & 0 \end{pmatrix}, \quad (\text{A2})$$

where

$$a = \langle \partial_{\lambda_1} \psi_{\boldsymbol{\lambda}} | \psi_{\boldsymbol{\lambda}} \rangle, \quad (\text{A3})$$

$$b = \langle \partial_{\lambda_2} \psi_{\boldsymbol{\lambda}} | \psi_{\boldsymbol{\lambda}} \rangle, \quad (\text{A4})$$

$$c = \langle \partial_{\lambda_1} \psi_{\boldsymbol{\lambda}} | \partial_{\lambda_2} \psi_{\boldsymbol{\lambda}} \rangle, \quad (\text{A5})$$

$$\alpha = \langle \partial_{\lambda_1} \psi_{\boldsymbol{\lambda}} | \partial_{\lambda_1} \psi_{\boldsymbol{\lambda}} \rangle, \quad (\text{A6})$$

$$\beta = \langle \partial_{\lambda_2} \psi_{\boldsymbol{\lambda}} | \partial_{\lambda_2} \psi_{\boldsymbol{\lambda}} \rangle. \quad (\text{A7})$$

-
- [1] G. Amelino-Camelia, The three perspectives on the quantum-gravity problem and their implications for the fate of lorentz symmetry, in *The Tenth Marcel Grossmann Meeting: On Recent Developments in Theoretical and Experimental General Relativity, Gravitation and Relativistic Field Theories (In 3 Volumes)* (World Scientific, 2005) pp. 2214–2216.
- [2] S. Weinstein and D. Rickles, Quantum Gravity, in *The Stanford Encyclopedia of Philosophy*, edited by E. N. Zalta and U. Nodelman (Metaphysics Research Lab, Stanford University, 2024) Spring 2024 ed.

- [3] I. Ciufolini, A. Paolozzi, E. C. Pavlis, R. Koenig, J. Ries, V. Gurzadyan, R. Matzner, R. Penrose, G. Sindoni, C. Paris, *et al.*, A test of general relativity using the lares and Lageos satellites and a GRACE Earth gravity model: Measurement of Earth's dragging of inertial frames, *The European Physical Journal C* **76**, 1 (2016).
- [4] M. Zych, L. Rudnicki, and I. Pikovski, Gravitational mass of composite systems, *Phys. Rev. D* **99**, 104029 (2019).
- [5] D. Moustos and C. Anastopoulos, Gravity-mediated decoherence, *Phys. Rev. D* **110**, 024022 (2024).
- [6] R. Y. Chiao, N. A. Inan, M. Scheibner, J. Sharping, D. A. Singleton, and M. E. Tobar, Gravitational Aharonov-Bohm effect, *Phys. Rev. D* **109**, 064073 (2024).
- [7] M. Carlesso, A. Bassi, *et al.*, Observable quantum entanglement due to gravity, *npj Quantum Information* **6**, 20 (2020), arXiv:1907.11696 [quant-ph].
- [8] T. Biswas, K. Lochan, and A. Raj, Inference of gravitational field superposition from quantum measurements, *Physical Review D* **108**, 084038 (2023), arXiv:2307.07583 [gr-qc].
- [9] J. Chen, Z. Wang, *et al.*, Detecting single gravitons with quantum sensing, *Nature Communications* **15**, 1794 (2024).
- [10] R. Colella, A. W. Overhauser, and S. A. Werner, Observation of gravitationally induced quantum interference, *Physical Review Letters* **34**, 1472 (1975-6-9).
- [11] H. Abele, G. Cronenberg, P. Geltenbort, T. Jenke, T. Lins, and H. Saul, qbounce, the quantum bouncing ball experiment, *Physics Procedia* **17**, 4 (2011), 2nd International Workshop on the Physics of fundamental Symmetries and Interactions - PSI2010.
- [12] T. Jenke, J. Bosina, G. Cronenberg, H. Filter, P. Geltenbort, A. N. Ivanov, J. Micko, M. Pitschmann, T. Rechberger, R. I. Sedmik, *et al.*, Testing gravity at short distances: Gravity resonance spectroscopy with qbounce, in *EPJ Web of Conferences*, Vol. 219 (EDP Sciences, 2019) p. 05003.
- [13] V. Nesvizhevsky, Gravitational quantum states of neutrons and the new GRANIT spectrometer, *Modern Physics Letters A* **27** (2012).
- [14] A. Landry and M. B. Paranjape, Gravitationally induced quantum transitions, *Phys. Rev. D* **93**, 122006 (2016).
- [15] B. Koch, E. Muñoz, and A. Santoni, Ultracold neutrons in the low curvature limit: Remarks on the post-newtonian effects, *Phys. Rev. D* **109**, 064085 (2024).
- [16] A. Ivanov, M. Wellenzohn, and H. Abele, Quantum gravitational states of ultracold neutrons as a tool for probing of beyond-riemann gravity, *Physics Letters B* **822** (2021).
- [17] C. Escobar, A. Martín-Ruiz, A. Escobar-Ruiz, and R. Linares, Testing the scalar sector of the standard-model extension with neutron gravity experiments, *European Physical Journal Plus* **137**, 1 (2022).
- [18] S. Sala, F. Castelli, M. Giammarchi, S. Siccardi, and S. Olivares, Matter-wave interferometry: towards antimatter interferometers, *Journal of Physics B: Atomic, Molecular and Optical Physics* **48**, 195002 (2015).

- [19] P. Perez, D. Banerjee, F. Biraben, D. Brook-Roberge, M. Charlton, P. Cladé, P. Comini, P. Crivelli, O. Dalkarov, P. Debu, *et al.*, The gbar antimatter gravity experiment, *Hyperfine Interactions* **233**, 21 (2015).
- [20] G. Cronenberg, H. Filter, M. Thalhammer, T. Jenke, H. Abele, and P. Geltenbort, A gravity of earth measurement with a qbounce experiment (2015), arXiv:1512.09134 [hep-ex].
- [21] Y. Himemoto, A. Nishizawa, and A. Taruya, Distinguishing a stochastic gravitational-wave signal from correlated noise with joint parameter estimation: Fisher analysis for ground-based detectors, *Phys. Rev. D* **107**, 064055 (2023).
- [22] A. Peters, K. Y. Chung, and S. Chu, High-precision gravity measurements using atom interferometry, *Metrologia* **38**, 25 (2001).
- [23] J. Gea-Banacloche, A quantum bouncing ball, *American Journal of Physics* **67**, 776 (1999).
- [24] V. Montenegro, Heisenberg-limited spin-mechanical gravimetry, *Phys. Rev. Res.* **7**, 013016 (2025).
- [25] J. Kohlrus, D. E. Bruschi, and I. Fuentes, Quantum-metrology estimation of spacetime parameters of the earth outperforming classical precision, *Phys. Rev. A* **99**, 032350 (2019).
- [26] H. Cramér, *Mathematical methods of statistics*, Vol. 9 (Princeton University Press, 1945).
- [27] M. G. A. Paris, Quantum estimation for quantum technology, *Int. J. Quantum Inf.* **7**, 125 (2009).
- [28] C. W. Helstrom, *Quantum detection and estimation theory* (Academic Press, 1976).
- [29] A. S. Holevo, *Probabilistic and Statistical Aspects of Quantum Theory*, 2nd ed. (Edizioni della Normale, Pisa, 2011).
- [30] J. Liu, X.-X. Jing, and X. Wang, Quantum metrology with unitary parametrization processes, *Sci. Rep.* **5**, 8535 (2015).
- [31] F. Albarelli, M. Barbieri, M. Genoni, and I. Gianani, A perspective on multiparameter quantum metrology: From theoretical tools to applications in quantum imaging, *Physics Letters A* **384** (2020).
- [32] J. Liu, H. Yuan, X.-M. Lu, and X. Wang, Quantum fisher information matrix and multiparameter estimation, *Journal of Physics A: Mathematical and Theoretical* **53**, 023001 (2020).
- [33] M. Wadati, The free fall of quantum particles, *Journal of the Physical Society of Japan* **68**, 2543 (1999).
- [34] X. He, R. Yousefjani, and A. Bayat, Stark localization as a resource for weak-field sensing with superheisenberg precision, *Phys. Rev. Lett.* **131**, 010801 (2023).
- [35] O. Vallée and M. Soares, *Airy functions and applications to physics*, Vol. 67 (World Scientific, 2004).
- [36] N. Wheeler, Classical/quantum dynamics in a uniform gravitational field, Nicholas Wheeler's Physics Lectures are owned by Reed College and archived by the Reed College Library. The original material is copyrighted by Nicholas Wheeler. (<https://www.reed.edu/physics/faculty/wheeler/documents/index.html>).
- [37] V. V. Nesvizhevsky, H. Börner, A. Gagarski, G. Petrov, A. Petukhov, H. Abele, S. Bäckler, T. Stöferle, and S. Soloviev, Search for quantum states of the neutron in a gravitational field: gravitational levels, *Nuclear Instruments and Methods in Physics Research Section A: Accelerators, Spectrometers, Detectors and Associated Equipment* **440**, 754 (2000).

- [38] M. A. Doncheski and R. W. Robinett, Expectation value analysis of wave packet solutions for the quantum bouncer: Short-term classical and long-term revival behaviors, *American Journal of Physics* **69**, 1084 (2001).
- [39] V. Nesvizhevsky, A. Petukhov, H. Börner, T. Baranova, A. Gagarski, G. Petrov, K. Protasov, A. Y. Voronin, S. Baeßler, H. Abele, *et al.*, Study of the neutron quantum states in the gravity field, *The European Physical Journal C-Particles and Fields* **40**, 479 (2005).
- [40] V. V. Nesvizhevsky, H. G. Börner, A. M. Gagarski, A. K. Petoukhov, G. A. Petrov, H. Abele, S. Baeßler, G. Divkovic, F. J. Rueß, T. Stöferle, A. Westphal, A. V. Strelkov, K. V. Protasov, and A. Y. Voronin, Measurement of quantum states of neutrons in the earth’s gravitational field, *Physical Review D* **67**, 10.1103/physrevd.67.102002 (2003).
- [41] H. Abele, S. Baeßler, and A. Westphal, Quantum states of neutrons in the gravitational field and limits for non-newtonian interaction in the range between 1 μm and 10 μm , in *Quantum Gravity* (Springer Berlin Heidelberg, 2003) p. 355–366.
- [42] G. Cronenberg, P. Brax, H. Filter, P. Geltenbort, T. Jenke, G. Pignol, M. Pitschmann, M. Thalhammer, and H. Abele, Acoustic rabi oscillations between gravitational quantum states and impact on symmetron dark energy, *Nature Physics* **14**, 1022 (2018).
- [43] R. L. Gibbs, The quantum bouncer, *American Journal of Physics* **43**, 25 (1975).
- [44] L. Seveso, V. Peri, and M. G. A. Paris, Quantum limits to mass sensing in a gravitational field, *Journal of Physics A: Mathematical and Theoretical* **50**, 235301 (2017).
- [45] L. Seveso and M. G. A. Paris, Can quantum probes satisfy the weak equivalence principle?, *Annals of Physics* **380**, 213 (2017).
- [46] J. A. Cañas, J. Bernal, and A. Martín-Ruiz, Exact classical limit of the quantum bouncer, *The European Physical Journal Plus* **137**, 1 (2022).
- [47] J. He and M. G. A. Paris, Scrambling for precision: optimizing multiparameter qubit estimation in the face of sloppiness and incompatibility, *arXiv preprint arXiv:2503.08235* (2025).
- [48] C. Cepollaro, F. Giacomini, and M. G. A. Paris, Gravitational time dilation as a resource in quantum sensing, *Quantum* **7**, 946 (2023).
- [49] Y. N. Obukhov, A. J. Silenko, and O. V. Teryaev, Manifestations of the rotation and gravity of the earth in high-energy physics experiments, *Phys. Rev. D* **94**, 044019 (2016).
- [50] R. Pierini, Effects of gravity on continuous-variable quantum key distribution, *Phys. Rev. D* **98**, 125007 (2018).
- [51] A. Candeloro, C. D. E. Boschi, and M. G. A. Paris, Quantum probes for universal gravity corrections, *Phys. Rev. D* **102**, 056012 (2020).
- [52] T. Chiba and S. Kinoshita, Quantum clocks, gravitational time dilation, and quantum interference, *Phys. Rev. D* **106**, 124035 (2022).
- [53] S. Razavian, M. G. A. Paris, and M. G. Genoni, On the quantumness of multiparameter estimation problems for qubit systems, *Entropy* **22** (2020).